Scattering of topological solitons on holes and barriers

Bernard Piette[1], W J Zakrzewski[1,2] and Joachim Brand[2]

[1] Department of Mathematical Sciences, University of Durham, Science Laboratories,
South Road, Durham DH1 3LE, UK
[2] Max Planck Institute for the Physics of Complex Systems, Nöthnitzer Straße 38,
01187 Dresden, Germany

Abstract
We study the scattering properties of topological solitons on obstructions in the
form of holes and barriers. We use the 'new baby Skyrme' model in $(2 + 1)$
dimensions and we model the obstructions by making the coefficient of the
baby Skyrme model potential–position dependent. We find that the barrier
leads to the repulsion of the solitons (for low velocities) or their complete
transmission (at higher velocities) with the process being essentially elastic.
The hole case is different; for small velocities the solitons are trapped while at
higher velocities they are transmitted with a loss of energy. We present some
comments explaining the observed behaviour.

PACS numbers: 11.10.Lm, 12.39.Dc, 03.75.Lm

1. Introduction

Consider a moving particle encountering a potential barrier or a potential hole. Then, the
barrier slows down the particle and if the energy of the particle is too low relative to the
barrier's height, the particle is reflected. In the potential hole case, the particle speeds up
in the hole and is always transmitted. However, consider now the same process in quantum
mechanics; then in both cases we have reflection and transmission, the relative magnitudes of
which depend on the parameters of the potential and on the energy of the particle.

Recently, some work has been done on the scattering properties of solitons of the nonlinear
Schrödinger model [1–4]. It was pointed out in [5] that the scattering of solitons at low
velocities resembles a classical particle in the sense that the soliton maintains its integrity
and follows a well-defined trajectory, with the difference that, nevertheless, the soliton can be
reflected by a potential hole. Such reflection is not possible in classical mechanics.

Motivated by these results, we have decided to look at this problem in the case of
topological solitons asking ourselves the question as to whether this case will resemble more
the classical particle case or the quantum mechanical systems?

To look at this more carefully, we have chosen to study this problem on the example of a (2 + 1)-dimensional system so that we could see the effects of the transverse direction and to allow for the radiation waves, if they are generated, to escape more easily. The model we have chosen is the baby Skyrme model discussed in detail in many publications [6, 7]. The mutual interactions of skyrmions in scattering events have been a topic of long standing interest and are summarized in [8–10]. Experimental realizations of topological solitons are possible in spinor Bose–Einstein condensates [11, 12].

The Lagrangian density of the 'baby Skyrme' model contains three terms from left to right: the pure S^2 sigma model, the Skyrme and the potential terms:

$$\mathcal{L} = \partial_\mu \vec{\phi} \cdot \partial^\mu \vec{\phi} - \theta_S[(\partial_\mu \vec{\phi} \cdot \partial^\mu \vec{\phi})^2 - (\partial_\mu \vec{\phi} \cdot \partial_\nu \vec{\phi})(\partial^\mu \vec{\phi} \cdot \partial^\nu \vec{\phi})] - V(\vec{\phi}), \quad (1)$$

where

$$V(\phi) = \mu(1 - \phi_3^2). \quad (2)$$

The vector $\vec{\phi}$ lies on the unit sphere S^2, hence $\vec{\phi} \cdot \vec{\phi} = 1$.

To have a finite potential energy, the field at spatial infinity is required to go to $\phi_3 = \pm 1, \phi_1 = \phi_2 = 0$. In this work, we choose 'the vacuum' to be defined as $\phi_3 = +1$.

Note that our boundary condition has defined a one-point compactification of R_2, allowing us to consider $\vec{\phi}$ on the extended plane $R_2 \bigcup \infty$ topologically equivalent to S^2. In consequence, the field configurations are maps

$$\vec{\phi} : S^2 \longrightarrow S^2, \quad (3)$$

which can be labelled by an integer-valued topological index Q:

$$Q = \frac{1}{4\pi} \int \vec{\phi} \cdot (\partial_x \vec{\phi} \times \partial_y \vec{\phi}) \, dx \, dy. \quad (4)$$

As a result of this nontrivial mapping, the model has topologically nontrivial solutions which describe 'extended structures', which have been called baby skyrmions. A soliton is then the simplest field configuration $\vec{\phi}$ corresponding to $Q = 1$ which minimizes the total energy and which can be calculated from $\mathcal{L}$ (1) by taking all terms in it with positive signs. This soliton field configuration has to be found numerically; however, as discussed in previous papers [6, 7], this problem reduces to having to solve an ordinary differential equation for a 'profile function' $f(r)$, where r is the radial distance from the position of the soliton.

Note that the soliton is exponentially localized and its asymptotic behaviour is controlled by μ.

In the next section, we describe a possible way of introducing an 'obstruction' into our model and discuss the results of our studies. In section 3, we present the results of our numerical simulations. Section 4 presents some concluding remarks.

2. Potential obstruction

There are various ways of introducing a potential hole or a potential barrier. However, given that the soliton field, strictly speaking, is never zero, even though it vanishes exponentially as we move away from its position, this potential has to be introduced in such a way that it does not change the 'tail' of the soliton, i.e. it has to vanish when $\phi_3 = 1$. A possible way to do this is to add an extra term to the Lagrangian which vanishes when $\phi_3 = 1$. Of course, there are many possible choices of such terms but given that our Lagrangian already contains a term with such a property we exploit this fact and choose to add $\alpha(1 - \phi_3^2)$ in some region of x and y. We choose this term to be independent of y so that the obstruction on the potential energy landscape, located in some finite region of x, say at positive x, resembles a trough in the 'hole'

case or a dam in the 'barrier' case. Then sending the soliton from a point well away from this obstruction, i.e. initially placed at some sufficiently negative x, in the positive x direction, we can study the effects of the obstruction.

In our numerical simulations, we have chosen the obstruction to be constant in a small range of x; this effectively corresponds to taking μ in the original Lagrangian to be given by μ_0 for x in the range of the obstruction and μ_1 elsewhere.

The case when $\mu_0 > \mu_1$ corresponds to a barrier (dam) and when $\mu_0 < \mu_1$ we have a hole (trough). We have performed many numerical simulations of such systems, varying both the sign and value of $\mu_0 - \mu_1$ and the velocity of the incoming soliton. We have also checked that, initially, the solitons were far enough from the obstruction so that the incoming solitons can be considered to be free.

In the next section, we present some results of our simulations. Both the cases of the hole and of the barrier have been studied and, as we shall see, they have produced very different results. The scattering by the barrier was found to be elastic, with hardly any radiation being generated in the process; by comparison the motion through the trough was inelastic with an interesting pattern of the decrease of velocity of the transmitted soliton.

3. Numerical simulations

3.1. General comments

We have performed most of our simulations on a 350×350 square grid with lattice spacing being 0.15. Thus, the lattice extended from -26.5 to $+26.5$ in each direction. The soliton was initially placed at $x = -12$, $y = 0$. Its size was determined by the choice of parameters, θ_s and μ which were chosen as $\theta_s = 0.5$ and $\mu_1 = 0.6$. This produced a soliton which was essentially localized to about 40 lattice points in each direction, i.e. to a region of 6×6 in real space. Thus, placing the soliton at $x = -12$ there was no problem with any boundary effects.

Next, we put our obstruction from $x = 0$ to $x = 30 \times 0.15 = 4.5$. We considered various values of the height of the obstruction. As they all led to qualitatively similar results, we performed most of our simulations for $\mu_1 - \mu_0 = 0.5$ and -0.1. The same is true when we varied the width of the barrier although changing the width changed the value of v_{cr}, the critical velocity above which the soliton is transmitted.

All our simulations were performed using a fourth order Runge–Kutta method with the field $\vec{\phi}$ being rescaled every few iterations. The time step of our simulations was taken to be 0.001. We used fixed boundary conditions and later we also used the absorbing boundary conditions at the edges of the lattice. This we generated by successively decreasing the magnitude of $\frac{d\vec{\phi}}{dt}$ at the last five rows and columns of the lattice.

To generate the time dependence, we calculated the initial configurations with the soliton located at $x = -12$ and $x = -11.9$ and we defined $\frac{d\vec{\phi}}{dt}$ as being proportional to the difference between these two $\vec{\phi}'$ orthogonalized with respect to $\vec{\phi}$ at $x = -12$. Varying the constant of proportionality we changed the initial velocity. This is an approximate way of introducing the initial condition corresponding to a moving soliton, which is a very good approximation for small values of velocities, when the relativistic effects are negligible. Using this method we have to calibrate the velocity—to check directly what the initial velocity is. Another way to proceed would involve introducing the correct time dependence into the initial ansatz (with Lorentz factors, etc) and then calculating $\frac{d\vec{\phi}}{dt}$ directly from this expression. Given the fact that the initial configurations are calculated numerically and involve some extrapolations we chose the easier option mentioned above. Our results show that our procedure was exceptionally
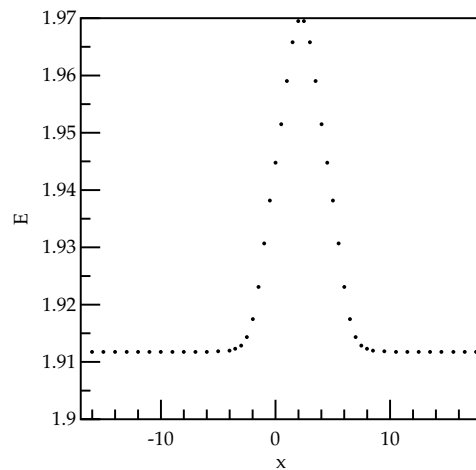
Figure 1. Energies of our basic soliton as a function of its position.

good; the moving soliton varied its height very little and it did not generate any perceptible amount of radiation.

3.2. Barrier

First, we have considered the effects of a barrier. Hence, between $x = 0$ and $x = 4.5$, we put $\mu_1 - \mu_0 = -0.1$. Then we placed the initial soliton at various values of x and calculated its energy without altering the shape of the soliton. This has told us what the barrier is like as seen by the soliton. The calculated energy plot is shown in figure 1.

We see that, although the original barrier is in the shape of a square barrier, the soliton perceives the barrier as a smooth hump or hill. This is, of course, due to the finite size of the soliton. As seen in figure 1, the barrier effects stretch from $x \sim -4$ to $x \sim 10$.

The soliton placed at $x = -12$ should be far away from the effects of the barrier. Next, we performed a series of simulations placing the soliton at $x = -12$ and sending it towards the barrier at various speeds. We have found extremely elastic behaviour in all cases. For low velocities ($v < v_{cr} \sim 0.2427$), the soliton bounced off the barrier while for $v > v_{cr}$ it was transmitted. At velocities close to v_{cr}, the soliton slowly climbed the ascending slope of the effective barrier of figure 1, either getting over it ($v > v_{cr}$) or falling back. In all the cases the process was elastic. This was seen through the plots of energy density, where we did not see any significant radiation energy. Also the values of the final velocity of the soliton were essentially the same as the initial ones, indicating that no significant energy loss had taken place. To calculate the initial velocity, we used the values of the time when the soliton reached $x = -5$ on the way towards the barrier. To calculate the final velocity, we used the times it reached $x = -5$ and $x = -11$ for the reflected soliton and $x = 11$ and $x = 21$ for the transmitted one. In this way, we were calculating the velocities in the region where there were no effects of the barrier. In figure 2, we plot the modulus of the outgoing versus incoming velocity. We note that the curve is essentially a straight line suggesting a simple linear relationship. In fact, the values of the incoming and outgoing velocities differ from each other in 3rd or 4th decimal points. So we can treat them as equal, within the numerical accuracy of our procedure.

The value of the critical velocity can be estimated by observing the trajectory of the soliton; if the soliton makes it to the 'top of the barrier', which is around $x \sim 2.25$, then it
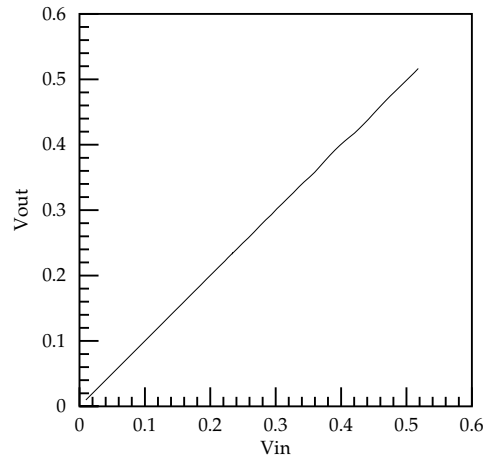
Figure 2. Soliton velocities, *x* axis—incoming, *y* axis—outgoing.
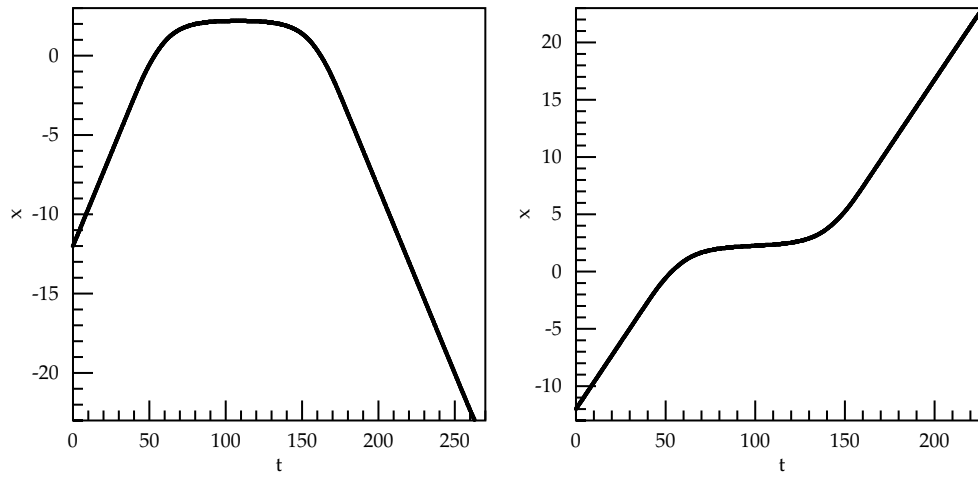

Figure 3. Time dependence of the position of the soliton initially placed at $x = -12$: left $v < v_{cr}$, right $v > v_{cr}$.

goes through, otherwise, it is reflected. In figure 3, we present plots of the time dependence of the soliton position in two cases: one corresponding to the velocity of just below the critical value, namely, $v \sim 0.2426$ and one just above at $v \sim 0.2428$.

We note that, in each case, the slopes of the curves before and after the soliton interacted with the barrier are the same. Thus, we see that the scattering is completely elastic; essentially no energy is lost during the climb of the barrier and because of this the velocity is unchanged, to the degree of accuracy of our calculation.

Looking at the static configuration with $\mu = 0.7$, we note that its energy is 1.968 which is exactly the energy that the incoming soliton has to have to be able to transfer all its kinetic energy into the potential energy—to be able to climb the barrier and transmitted. Thus, v_{cr} is determined by the energy that the incoming soliton corresponding to $\mu = 0.6$ has to have so that its energy corresponds to the energy of the static soliton of $\mu = 0.7$.
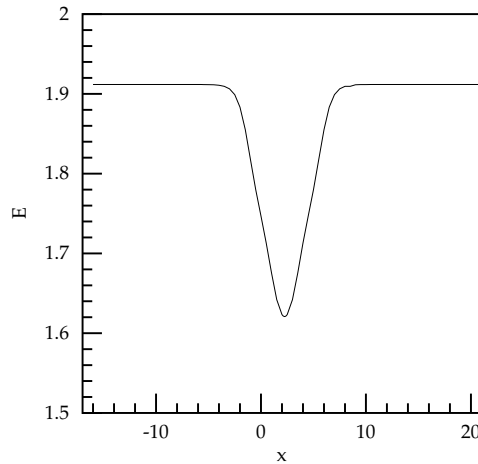
Figure 4. Energies of our basic soliton as a function of its position.

Note that one can give the following nonrelativistic argument which supports our claims. First, note that the mass of the soliton is given by the total energy ($c = 1$) so $M \sim 1.912$. Then, $\frac{M v_{cr}^2}{2} \sim 1.912 \times 0.058\,903\,29/2 = 0.056\,31$ which is in agreement with the difference of energies $\delta E = 1.968 - 1.1912 \sim 0.056$.

This assumes an elastic behaviour and this is what we have seen in our numerical simulations. Thus, in the case of the bump, the whole kinetic energy of the incoming soliton is converted into the potential energy of the soliton at the top of the barrier and then the soliton can be transmitted elastically.

3.3. Hole

We placed the hole in the same place as the barrier and we took $\mu_1 - \mu_0 = 0.5$. Next, as in the barrier case, we placed the initial soliton at various values of x and calculated its energy. This has told us what the hole is like as seen by the soliton. The calculated energies are shown in figure 4. Once again we see that the effective hole as seen by the soliton is quite smooth. We have performed many simulations and have found that, again, there exists a critical velocity v_{cr}. Above v_{cr} the soliton is transmitted and below it falls in and gets trapped in the hole.

The critical velocity is around $v_{cr} \sim 0.155$. Solitons started off from $x = -12$ fall into the hole and stay there oscillating and gradually losing their energy by emitting radiation. Two typical trajectories are shown in figure 5. The left picture shows a trapped soliton with initial velocity $v \sim 0.09$, i.e. below v_{cr}, and the right one shows a transmitted soliton with initial velocity $v \sim 0.16$.

For velocities above v_{cr} we have a transmission, but this time the outgoing soliton is much slower. In figure 6, we present the plot of the outgoing velocities as a function of the incoming ones.

We not only note the significant decrease of the velocity, but also the oscillations in the values of the outgoing velocities.

We have looked at the details of the scattering, but we have not succeeded in revealing the origin of the oscillations. We have rerun some simulations with absorption of the waves at the boundaries; the results were essentially the same suggesting that the origin of the oscillations has nothing to do with any waves of emitted radiation bouncing off the boundaries.
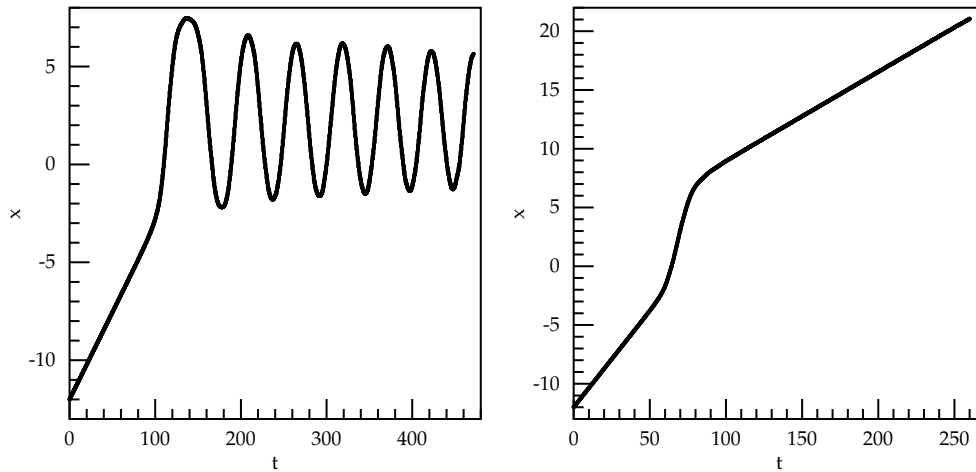
Figure 5. Time dependence of the position of the soliton initially placed at $x = -12$: left, $v < v_{cr}$; right, $v > v_{cr}$.
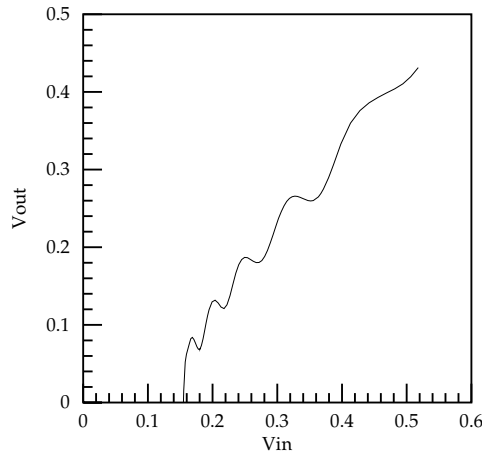

Figure 6. Velocities of transmitted solitons, x axis—incoming, y axis—outgoing

Thus, the origin of the effect is associated with the interaction of the soliton with the hole and the emission of the radiation during this process. To check this, we have looked at the time spent in the hole and its relation to the time needed for the soliton to traverse the hole had the soliton moved with the initial or the final velocity.

In figure 7(*a*), we plot the time spent by the soliton in the hole as a function of the incoming velocity. In figure 7(*b*), we plot three curves: all as a function of the initial velocity. They present the difference of the time the soliton spent in the hole from which is subtracted the time needed to traverse the hole with the initial velocity, the same with the final velocity and the same with the average velocity.

We see a dramatic difference in all three expressions.

It is clear that the time in the hole is related to the oscillations of the velocities. It is also clear that as the incoming velocity is much higher than the outgoing velocity the expression for the time spent in the hole, the time needed to traverse the hole at a given velocity, is the
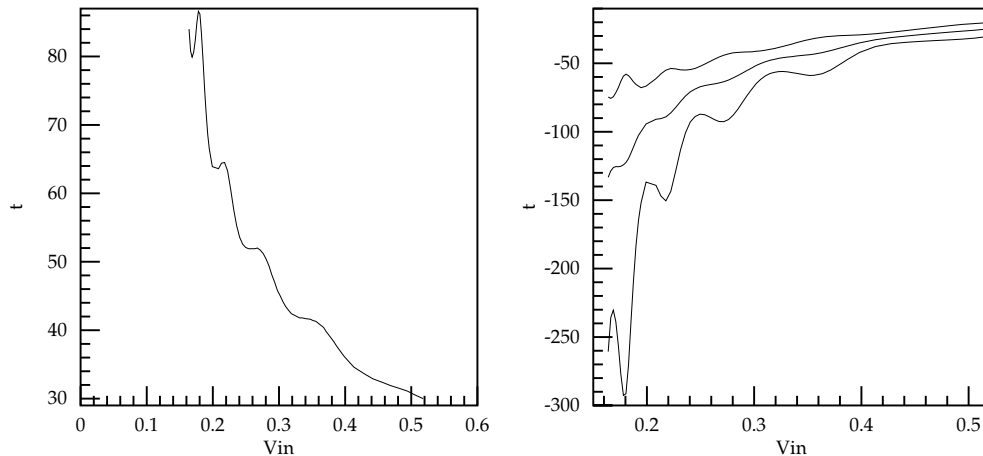
Figure 7. Left: time spent in the hole; right: time in the hole minus the time needed to traverse the hole with various velocities. Top curve: initial velocity, middle curve: average, bottom curve: outgoing one.
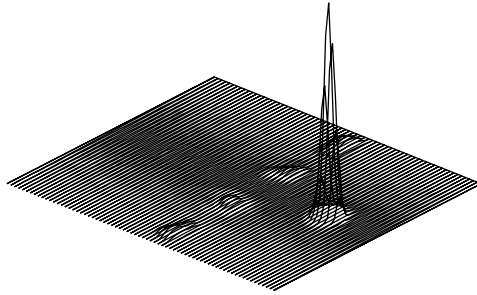

Figure 8. The density of the kinetic energy in a simulation just after the soliton has passed the hole. $T = 150$, $v_{in} = 1.9165$.

lowest when we take the largest velocity, i.e. the incoming velocity. It is also clear that the potential hole increases the velocity—so all our expressions in figure 7(*b*) are negative.

Looking at the curves in figure 7(*b*), we see that the oscillations in outgoing velocity are pretty much reproduced by the time spent by the soliton in the hole and almost eliminated when we take the middle curve in figure 7(*b*). This suggests that during the motion through the hole the soliton velocity changes in a complicated way (gradually producing the oscillations). If, in the plots in figure 7(*b*), we use the initial velocity the oscillations show up in the difference of times; if we use the final velocity we overcompensate and we have the opposite oscillations; taking the average velocity accounts for most of the oscillations leaving a curve which is much smoother. This curve, however, does show the extra velocity in the hole, which of course is related to the incoming velocity.

Looking at the curve, we note that its features are as expected; we note a slow rise with the increase of v_{inc}, which is consistent with the loss of energy in the hole.

Note that this time the process is very different from the situation of a barrier. In the barrier case, the incoming soliton has some kinetic energy which it has to convert to the potential one to rise up the barrier. This seems to be done elastically with essentially no radiation. In the hole case, the soliton has a kinetic energy and as it moves into the hole it gains extra energy

as well. This time the extra energy is partially converted into the increased speed of motion but some of it is got rid of via radiation. In fact, this is what we have seen in our numerical simulations which did show some radiation. Then, when it reaches the other side of the hole and it starts 'climbing out of the hole' the soliton may not have enough energy to get out. Hence, for low speeds it gets trapped in the hole.

Of course, we do not really understand why the soliton does not convert all its extra energy into the increased kinetic energy and why the velocities give us the very interesting patterns that can be seen from the plot in figure 6. Clearly, there must be an internal mode of the soliton that gets excited and which radiates the excess energy.

This point requires further study.

4. Conclusions

We have looked at a system involving a topological soliton in two dimensions and a potential, of both a barrier and a hole type.

When the soliton was sent towards the barrier its behaviour resembled that of a particle. Thus at low energies the soliton was reflected by the barrier and at higher energy it was transmitted. The scattering process was very elastic. During the scattering the kinetic energy of the soliton was gradually converted into the energy needed to 'climb the barrier'. If the soliton had enough energy to get to the 'top' of the barrier then it was transmitted, otherwise it slid back regaining its kinetic energy.

Note that the soliton size is related to the parameters of the model and so depends on μ. Hence, during the climb of the barrier, the soliton altered its size (it decreased a little)—to fit the local value of μ; when it got through, or slipped back, its size returned to it original value. This is what one would expect in an elastic scattering and this is what we saw in the numerical simulations. In fact, the soliton size oscillated a little, around its 'correct' value and the amplitude of these oscillations has not changed much during the scattering process and the final oscillations resembled the original ones.

In the hole case, the situation was very different. This time, the soliton gained an extra energy as it entered the hole. Some of this energy was converted into kinetic energy of the soliton, some was radiated away. So when the soliton tried to 'get out' of the hole it had less kinetic energy than at its entry and when this energy was too low it remained trapped in the hole. During the scattering process, like in the case of a barrier, the soliton size changed and its oscillations increased significantly. Afterwards they stayed like this—with much higher amplitude of oscillations than before. Hence, the increase in oscillations is related to the inelasticity of the process and the emitted radiation.

The scattering of a topological soliton on a hole is thus reminiscent of a classical particle under the influence of friction. We have not found any indication of nonclassical reflection as in the case of nonlinear Schrödinger solitons [5]. However, in contrast to a classical particle with simple velocity-dependent friction, we have found interesting oscillations hinting at some underlying resonant mechanism.

We have looked in detail at the behaviour of the solitons during their scattering process and, so far, have not found a satisfactory explanation of the observed 'oscillations' in the outgoing velocities (in the case of transmission by the hole).

Clearly, this is related to the properties of the radiation—the only plausible explanation we can find is that the radiation is sent out in separate bursts. This is very much what we saw in the actual simulations. In figure 8, we present a plot of the density of the kinetic energy seen in a typical simulation.

Looking at the plot, we see distinctive waves of energy moving along the 'trough' (i.e., in the *y* directions). The 'high' peak is the kinetic energy density of the moving soliton.

Clearly, we need to find an explanation of the observed radiation pattern. But, this lies outside the scope of this paper.

Acknowledgments

References

[1] Cao X D and Malomed B A 1995 *Phys. Lett.* A **206** 177
[2] Goodman R H, Holmes P J and Weinstein M I 2004 *Physica* D **192** 215
[3] Sakaguchi H and Tamura M 2004 *J. Phys. Soc. Japan* **73** 503
[4] Miroshnichenko A E, Flach S and Malomed B 2003 *Chaos* **13** 874
[5] Lee Ch and Brand J 2005 *Preprint* cond-mat/0505697
[6] Weidig T 1999 *Nonlinearity* **12** 1489–503
[7] Piette B M A G and Ward R S 2005 *Physica* D **201** 45–55
[8] Manton N and Sutcliffe P 2004 *Topological Solitons* (Cambridge: Cambridge University Press)
[9] Peyrard M, Piette B and Zakrzewski W J 1992 *Nonlinearity* **5** 563–83
[10] Piette S B, Kudryavtsev A and Zakrzewski W J 1998 *Nonlinearity* **11** 783–96
[11] Matthews M R *et al* 1999 *Phys. Rev. Lett.* **83** 2498
[12] Al Khawaja U and Stoof H 2001 *Nature* **411** 918